Ultra-high precision determination of site energy differences using a Bayesian method

Journal Item

PHYSICAL REVIEW B **89**, 121405(R) (2014)

Ultra-high precision determination of site energy differences using a Bayesian method

B. A. J. Lechner,[1,*] P. R. Kole,[1] H. Hedgeland,[1,†] A. P. Jardine,[1] W. Allison,[1] B. J. Hinch,[2] and J. Ellis[1,‡]

[1]*Cavendish Laboratory, University of Cambridge, JJ Thomson Avenue, Cambridge CB3 0HE, United Kingdom*

[2]*Department of Chemistry and Chemical Biology, Rutgers University, Piscataway, New Jersey 08854, USA*

(Received 12 April 2013; revised manuscript received 5 February 2014; published 10 March 2014)

Accurate experimental data of adsorbate potential energy landscapes are crucial as benchmarks for the evaluation of first-principles calculations. Here, we present a Bayesian method, analyzing the difference in forward and backward hopping rate in helium spin-echo measurements, that allows us to determine the binding-energy difference between two sites with unprecedented accuracy. Demonstrating the power of the method on the model system cyclopentadienyl/Cu(111), we find an energy difference between fcc and hcp hollow sites of (10.6 ± 1.7) meV.

DOI: 10.1103/PhysRevB.89.121405 PACS number(s): 68.35.Ja, 68.43.Fg, 68.43.Jk, 68.49.Bc

As theorists strive to reach "chemical accuracy" with state-of-the-art calculation methods [1–3], it is increasingly important to obtain high-precision experimental results that can be used as definitive benchmark data to evaluate these methods [4–7]. In many fields of science and technology, the development of ever more accurate *ab initio* theoretical methods significantly reduces the time required to tailor and characterize new materials. Applications in the organic electronics industry, for example, continuously increase the need for a fundamental understanding of thin-film growth [8–12], a process that can be accelerated significantly through the development of accurate *ab initio* theoretical methods. In recent years, progress has been made by including van der Waals corrections to density functional theory, providing valuable information about adsorbate–substrate interactions through binding-energy differences between local adsorption minima [13–16]. The experimental determination of such energy differences for the testing of theoretical methods, however, is difficult and few results have been reported to date.

From the temperature and coverage dependence of infrared reflection absorption spectroscopy (IRAS) [17] and electron energy-loss spectroscopy (EELS) [18] data, for example, the energy difference between CO adsorbed at top and hollow sites on Ni(111) was determined to be (36 ± 6) meV at a coverage, θ, of 0.14 monolayers (MLs) and (41 ± 7) meV at $\theta = 0.13$ ML, where one ML is defined as one adsorbate molecule per substrate atom. For CO adsorbed on the top and bridge sites of Pt(111) the site energy difference was deduced from x-ray photoemission spectroscopy (XPS) data to be (41 ± 7) meV for $\theta < 0.35$ ML [19]. However, a re-analysis of the XPS data including lateral interactions yielded a much higher site energy difference of (95 ± 15) meV [20]. The present work presents an enhanced approach, using a Bayesian method, to determine site energy differences from experimental data with much higher accuracy than previously possible.

Helium spin-echo (HeSE) spectroscopy follows atomic *motion* on picosecond time and atomic length scales and as such is a much more sensitive probe of potential energy surfaces (PES) and lateral interactions than probes of static structure [21–24]. HeSE measurements of the same system, CO/Pt(111), showed that the strong pairwise CO–CO interactions used in the re-analysis of the XPS data are in fact absent, and more complex many-body interactions are required [25]. HeSE is therefore in the unique position not only of being able to measure with much higher accuracy, but also reliably determine the lateral interactions that are so important in interpreting experimental data. In another recent example, studying CO/Cu(111), not only the preferred adsorption site and barrier to diffusion, but also the shape of the energy landscape around the transition state could be determined [26]. A PES is usually obtained by modeling the experimental data in molecular dynamics (MD) simulations [24,26]. In addition, in the limit of weak interactions and high friction, analytical models provide a good description of HeSE data [27,28]. Herein, we present a study of the energy difference between two adsorption sites with unprecedented accuracy, through an analysis of the differential hopping rate between the sites. The result thus arises directly from analysis of the experimental data rather than by modeling the data, which inevitably allows some degree of "trade-off" between the various parameters. Furthermore, the possibility of testing theoretical calculations on the precisely determined adsorption energy difference between two specific high-symmetry points rather than the general agreement with a full PES can be of great value for advancing computationally expensive techniques.

The method we present is universally applicable to any moving adsorbate system that can be studied with HeSE. Here, we demonstrate its power for 0.03 ML cyclopentadienyl (Cp), C_5H_5, on Cu(111), a model system which has been characterized in detail in a previous HeSE study [29]. We extend our earlier room-temperature study to 135 K where we are more sensitive to detecting small energy differences between adsorption sites. Due to the exceptionally weak lateral interadsorbate interactions and the high friction typical for molecular adsorbates [30], giving predominantly single jumps, the Cp/Cu(111) system allows us to present the Bayesian method in its purest form, employing analytical models for jump diffusion. We would like to emphasize, however, that the method is not restricted to high-friction and weak-interaction

*Present address: Materials Sciences Division, Lawrence Berkeley National Laboratory, Berkeley, California 94720, USA; bajl2@cam.ac.uk

†Present address: London Centre for Nanotechnology, University College London, London WC1H 0AH, United Kingdom.

‡je102@cam.ac.uk

systems. More complex systems, such as diffusing hydrogen atoms, may be analyzed by replacing the analytical lineshapes with forms derived from MD or Monte Carlo site-to-site hopping simulations [31].

The HeSE technique probes surface dynamics by measuring the loss in correlation of the positions of adsorbates with time [21,32]. A beam of helium-3 atoms is spin polarized and split into two components of opposite nuclear spins. The two components scatter from the sample surface separated by a time delay, t, before they are recombined and spin analyzed. Motion that occurs during t results in a reduction of the correlation between the two beam components and thus in a loss of polarization measured in the detector. For aperiodic diffusion the polarization typically decays exponentially with time, while static defects, or confined diffusion, cause a constant level to which the polarization decays, giving the intermediate scattering function (ISF) of the form $a \cdot \exp(-\alpha t) + c$. To map out two-dimensional surface diffusion we study the decay rate, α, as a function of momentum transfer parallel to the surface, $\Delta \boldsymbol{K}$, and along two azimuths.

In our prior investigation of the Cp/Cu(111) dynamics we found that the molecule adsorbs preferentially on fcc and hcp hollow sites, hopping over an effective activation barrier of (41 ± 1) meV [29]. On the Cu(111) lattice, the two different types of hollow sites form a non-Bravais lattice with different jump directions for species originating at fcc and hcp sites, respectively, as illustrated in Fig. 1(a). The resulting experimental lineshapes are a sum of two exponentials,

$$\mathrm{ISF}(t) = a_1 \cdot \exp(-\alpha_1 t) + a_2 \cdot \exp(-\alpha_2 t). \qquad (1)$$

Analytical models for jump diffusion on degenerate fcc and hcp sites predict a single exponential lineshape along the $\langle 1\bar{1}0 \rangle$ azimuth and two exponentials along $\langle 11\bar{2} \rangle$ at certain momentum transfer values; nondegeneracy, however, results in a change in the ratio of the two decays along $\langle 11\bar{2} \rangle$ and the appearance of a second exponential along $\langle 1\bar{1}0 \rangle$, growing in intensity as the energy difference between fcc and hcp sites, ΔE, increases [27]. In the past, HeSE experiments were analyzed by investigating each ISF individually [22,26]. Using that methodology, we found the lineshapes along $\langle 1\bar{1}0 \rangle$ at 300 K exhibited little evidence for double decays, and estimated that fcc and hcp hollow sites are approximately degenerate [29]. Here we show how a Bayesian analysis can be employed to obtain a more accurate determination of ΔE, confirming that the energy difference is indeed small, yet nonzero.

Adsorbate diffusion between fcc and hcp sites is determined by the jump frequencies, ν_1 and ν_2, from one site to an adjacent one. Figure 1(b) shows the energy landscape along the diffusion pathway and defines the jump rates. In the analytical model for jump diffusion between fcc and hcp sites [27], the ISF is determined by two variables: the mean residence time, τ, in site 1, which is the inverse of the total jump rate out of site 1, ν_1, and λ, the differential jump rate between sites 1 and 2, ν_1/ν_2. At a given $\Delta \boldsymbol{K}$ value, the relative intensity of the two exponentials, a_1/a_2, and the relative decay rates, α_1/α_2, are fixed for each combination of λ and τ, defined by the equations given in Ref. [27]. The jump rate is defined by

$$\nu = \frac{1}{\tau} = \Gamma_0 \cdot \exp\left(-\frac{E}{k_B T}\right), \qquad (2)$$

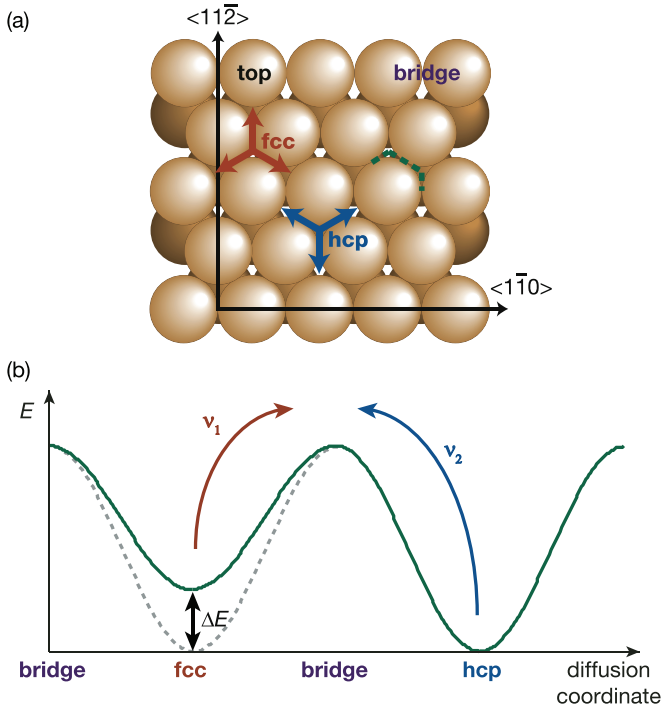

FIG. 1. (Color online) Jump diffusion on a Cu(111) surface. (a) The four high-symmetry sites, jump vectors connecting fcc and hcp sites, and the two principal crystal directions. (b) Schematic illustration of a cross section of the PES along the path of diffusion for Cp, marked as the dashed line in (a), defining ΔE as the energy difference between fcc and hcp sites, and ν_1 and ν_2 as the jump frequencies from fcc to hcp sites and vice versa. Note that our experiments do not allow us to determine which hollow site has the lower adsorption energy.

where k_B is the Boltzmann constant, T is the temperature, and Γ_0 is a prefactor related to the vibrational frequency at the adsorption site and the friction. Hence, λ can be written as

$$\lambda = \frac{\nu_1}{\nu_2} = \frac{\Gamma_{0,1} \cdot \exp\left(-\frac{E_1}{k_B T}\right)}{\Gamma_{0,2} \cdot \exp\left(-\frac{E_2}{k_B T}\right)} = \Gamma_R \exp\left(\frac{\Delta E}{k_B T}\right), \qquad (3)$$

with two unknown quantities: ΔE and Γ_R, the ratio of the values of Γ_0 at the two hollow sites. By determining λ and τ at two or more temperatures, Γ_R and ΔE may be determined, using Arrhenius' law.

Two developments allow us to determine ΔE with high accuracy: first, we have extended earlier measurements to lower temperatures, where the difference in forward and backward hopping rate is more marked due to the temperature dependence of λ, giving greater sensitivity in measuring ΔE; and second, we employ a Bayesian method [33], in a global analysis, using measurements over a wide range of $\Delta \boldsymbol{K}$. Rather than analyzing each ISF separately, a Bayesian method searches for the probability that a model describes all ISFs correctly. To identify λ at each temperature, we find the relative probability that λ and τ have particular values given all the ISFs measured at that temperature. We then integrate out τ over its range to leave the relative probability of λ as a function of λ, and hence the most likely value of λ and an error estimate on this value given the data.

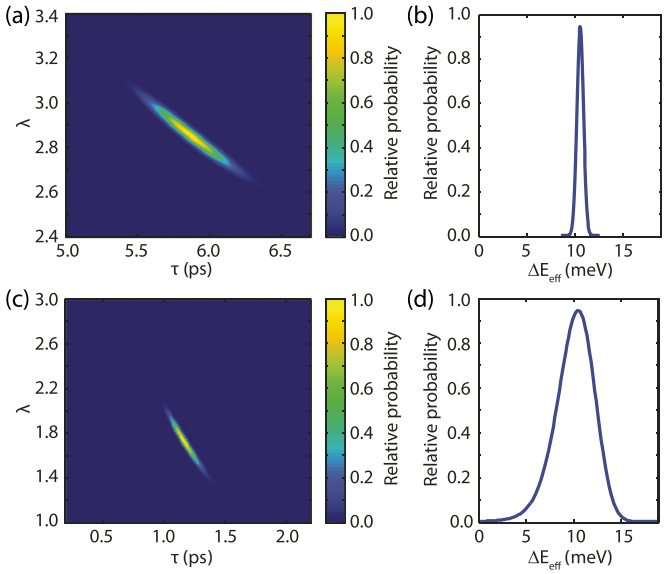

FIG. 2. (Color online) Probability distribution probing the $\lambda-\tau$ space for Cp hopping between fcc and hcp sites on Cu(111), at (a) 135 K and (c) 300 K. A clear peak is observed at both temperatures. By marginalizing over τ and calculating an effective energy difference between the two sites, ΔE_{eff}, from λ, we obtain the probability distribution of ΔE_{eff} at (b) 135 K and (d) 300 K.

Central to the Bayesian method is Bayes' theorem [33],

$$P(M|D) = \frac{P(D|M)P(M)}{P(D)}, \tag{4}$$

which states that the desired quantity—the probability $P(M|D)$ that a proposed model M is correct given the data D—is proportional to the probability that the data would have been produced if the model were correct, $P(D|M)$, which can be calculated easily.[1] We can thus compare relative probabilities of different models, or different values of λ and τ.

The procedure we apply is as follows: we first propose values for the variables λ and τ and calculate the prefactors a_1 and a_2 and exponents α_1 and α_2 from the analytical models given in Ref. [27]. We then obtain the lineshape of the model ISF for a particular intensity, A, and constant level, C, through

$$M = A[a_1 \cdot \exp(-\alpha_1 t) + a_2 \cdot \exp(-\alpha_2 t)] + C \tag{5}$$

and calculate the probability that the measured ISF would be produced by the model. We further marginalize (integrate) over all relevant values of A and C, giving the probability that this specific measured ISF would be obtained for the selected values of λ and τ. For this marginalization, we employ an analytical formula that makes the whole fitting procedure fast enough to be performed on a desktop-grade computer, which is described in the Supplemental Material. [34] Finally, we take the product of the probability distributions of all measured spectra to obtain the probability that the entire data set is given by the model for the selected λ and τ values. Bayes' theorem, shown in Eq. (4), states that the total probability $P(D|M)$, which we have calculated, is directly proportional to the probability that the values for λ and τ are correct, given our data.

The analytical models for hopping on a non-Bravais lattice of hollow sites show that double decay lineshapes are most strongly marked at $\Delta\boldsymbol{K} > 1.0$ Å^{-1} along the $\langle 11\bar{2}\rangle$ azimuth [27]. We therefore use the data in that region in our statistical analysis, giving a clear peak in the probability distribution of each spectrum. It should be noted that we check all fits visually and do not observe any trends in the optimum rate λ with $\Delta\boldsymbol{K}$, suggesting that the probability distributions of all ISFs can be combined to give a single model to describe the data set. Figures 2(a) and 2(c) show the total probability distributions for all spectra analyzed at 135 K and 300 K, respectively, giving maximum probability for $\lambda = 2.86$ and $\tau = 5.86$ ps at 135 K and $\lambda = 1.73$ and $\tau = 1.16$ ps at 300 K. The results can be marginalized over τ by integrating the probability over τ for a particular value of λ [33], providing a standard deviation for λ through the peak width. The maximum probability is found for $\lambda = 2.85 \pm 0.07$ at 135 K and $\lambda = 1.73 \pm 0.13$ at 300 K. We then used these two values for λ to calculate $\Gamma_R = 1.15 \pm 0.16$ and $\Delta E = 10.6 \pm 1.7$ meV

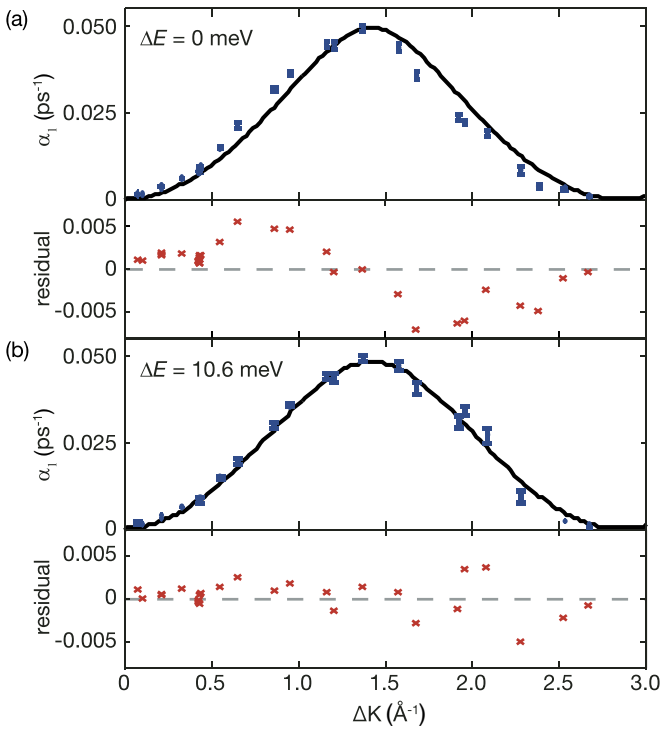

FIG. 3. (Color online) Comparison of the description of the HeSE measurements for 0.03 ML Cp/Cu(111) at 135 K along $\langle 11\bar{2}\rangle$ by (a) a model with degenerate fcc and hcp sites and (b) a model with $\Delta E = 10.6$ meV. The points in the respective top panels show the variation of the slow decay, α_1, with $\Delta\boldsymbol{K}$ while the solid lines illustrate the predicted $\alpha_1(\Delta\boldsymbol{K})$ dependence for the two models. Note that α_2 is given through α_1, hence we only show α_1 for simplicity. The bottom panels give the residuals after subtracting the analytical model from the points. A clear deviation from the model is observed for (a) $\Delta E = 0$ meV, with all points systematically above the model lines at low $\Delta\boldsymbol{K}$ and below the lines at high $\Delta\boldsymbol{K}$. Including an energy difference of 10.6 meV gives points evenly scattered around the model lines.

[1]The probability of getting the data, $P(D)$, and the prior probability of the model, $P(M)$, are constant.

through Eq. (3). As originally estimated from the shape of individual ISFs [29], ΔE is small, yet non-negligible, compared to the effective activation barrier for diffusion, which is (41 ± 1) meV. In Figs. 2(b) and 2(d) we plot the marginalized probability at each temperature as a function of an effective site energy difference, $\Delta E_{\text{eff}} = k_B T \ln(\lambda/\Gamma_R)$, derived assuming Γ_R has its most likely value, 1.15, to illustrate the precision of the measurements at the two temperatures. The smaller uncertainty at 135 K illustrates that the site energy difference has a greater effect on the hopping rates at lower temperatures.

To support the conclusions of the Bayesian analysis, we now illustrate the improved description of the HeSE data afforded by including ΔE explicitly in a conventional (decay constant as a function of momentum transfer) analysis of the measurements at 135 K along the $\langle 11\bar{2} \rangle$ direction. Using a least-squares algorithm, the data are fitted for a particular value of ΔE, and hence λ, by Eq. (1) and a constant term c, where the ratios a_1/a_2 and α_1/α_2 are defined by the analytical model used to interpret the data, leaving three free parameters, a_1, α_1, and c. Figure 3 compares the description of the low-temperature data by a model for (a) $\Delta E = 0$ and (b) $\Delta E = 10.6$ meV, showing the resulting α_1 values in the respective top panels and the residual after subtracting the analytical model from α_1 below. As the ratio α_1/α_2 is determined by ΔE, the analysis of the same experimental data with different values of ΔE results in somewhat different values of α_1 (and α_2), observed as a slight shift in the points shown in panels (a) and (b) [27]. The necessity to interpret the data with the correct energy difference can be seen clearly from the accuracy with which the solid lines representing the analytical model describe the points from the experimental data. When we assume degenerate sites, points lie systematically above the lines at low $\Delta \boldsymbol{K}$ and below the lines at high $\Delta \boldsymbol{K}$. Accounting for a small energy difference of 10.6 meV, however, gives a much improved description of the data. Specifically, the decay rates follow the predicted lines much more accurately and the residuals are scattered more evenly around zero.

In summary, our Bayesian analysis of the diffusion of an organic adsorbate provides ultra-high precision information on the energy difference between two adsorption sites. From our HeSE experiments, we conclude that cyclopentadienyl moves in single jumps between fcc and hcp sites that are energetically different by $\Delta E = (10.6 \pm 1.7)$ meV. We have demonstrated that the description of the behavior at low temperatures is much improved by taking into account this small adsorption energy difference, supporting the results from our statistical analysis.

Our approach offers a simple but powerful test of theoretical models, of general applicability to organic and other mobile adsorbate species. The possibility of validating computationally expensive calculations by the precise determination of the energy difference between two high-symmetry points is an important step towards the development and validation of new calculation methods.

Financial support by the EPSRC (EP/E0049621), the Austrian Academy of Sciences (B.A.J.L.), the Royal Society (A.P.J.), and the US National Science Foundation (CHE1124879, B.J.H.) is gratefully acknowledged.

[1] K. Reuter, D. Frenkel, and M. Scheffler, Phys. Rev. Lett. **93**, 116105 (2004).
[2] G. Csányi, T. Albaret, M. C. Payne, and A. De Vita, Phys. Rev. Lett. **93**, 175503 (2004).
[3] J. Klimeš, D. R. Bowler, and A. Michaelides, J. Phys.: Condens. Matter **22**, 022201 (2010).
[4] G. Mercurio, E. R. McNellis, I. Martin, S. Hagen, F. Leyssner, S. Soubatch, J. Meyer, M. Wolf, P. Tegeder, F. S. Tautz, and K. Reuter, Phys. Rev. Lett. **104**, 036102 (2010).
[5] M. Sacchi, S. Jenkins, H. Hedgeland, A. P. Jardine, and B. J. Hinch, J. Phys. Chem. C **115**, 16134 (2011).
[6] B. A. J. Lechner, H. Hedgeland, J. Ellis, W. Allison, M. Sacchi, S. J. Jenkins, and B. J. Hinch, Angew. Chem. Int. Ed. **52**, 5085 (2013).
[7] M. Callsen, N. Atodiresei, V. Caciuc, and S. Blügel, Phys. Rev. B **86**, 085439 (2012).
[8] G. Witte and C. Wöll, J. Mater. Res. **19**, 1889 (2004).
[9] Z. Liu, M. Kobayashi, B. C. Paul, Z. Bao, and Y. Nishi, Phys. Rev. B **82**, 035311 (2010).
[10] N. Atodiresei, J. Brede, P. Lazić, V. Caciuc, G. Hoffmann, R. Wiesendanger, and S. Blügel, Phys. Rev. Lett. **105**, 066601 (2010).
[11] V. Vardeny, Nat. Mater. **8**, 91 (2009).
[12] J. V. Barth, G. Costantini, and K. Kern, Nature (London) **437**, 671 (2005).
[13] S. J. Clark, M. D. Segall, C. J. Pickard, P. J. Hasnip, M. J. Probert, K. Refson, and M. Payne, Z. Kristallogr. **220**, 567 (2005).
[14] J. Klimeš and A. Michaelides, J. Chem. Phys. **137**, 120901 (2012).
[15] A. Tkatchenko, R. A. DiStasio, Jr., R. Car, and M. Scheffler, Phys. Rev. Lett. **108**, 236402 (2012).
[16] S. Jenkins, Proc. R. Soc. A **465**, 2949 (2009).
[17] A. Beniya, N. Isomura, H. Hirata, and Y. Watanabe, Surf. Sci. **606**, 1830 (2012).
[18] S. Tang, M. Lee, Q. Yang, J. Beckerle, and S. Ceyer, J. Chem. Phys. **84**, 1876 (1986).
[19] M. Kinne, T. Fuhrmann, C. Whelan, J. Zhu, J. Pantförder, M. Probst, G. Held, R. Denecke, and H.-P. Steinrück, J. Chem. Phys. **117**, 10852 (2002).
[20] J.-S. McEwen, S. Payne, H. J. Kreuzer, M. Kinne, R. Denecke, and H.-P. Steinrück, Surf. Sci. **545**, 47 (2003).
[21] A. P. Jardine, H. Hedgeland, G. Alexandrowicz, W. Allison, and J. Ellis, Prog. Surf. Sci. **84**, 323 (2009).
[22] H. Hedgeland, P. Fouquet, A. P. Jardine, G. Alexandrowicz, W. Allison, and J. Ellis, Nat. Phys. **5**, 561 (2009).
[23] A. P. Jardine, J. Ellis, and W. Allison, J. Phys.: Condens. Matter **14**, 6173 (2002).
[24] J. Ellis, A. P. Graham, F. Hofmann, and J. P. Toennies, Phys. Rev. B **63**, 195408 (2001).
[25] G. Alexandrowicz, P. R. Kole, E. Y. M. Lee, H. Hedgeland, R. Ferrando, A. P. Jardine, W. Allison, and J. Ellis, J. Am. Chem. Soc. **130**, 6789 (2008).
[26] P. R. Kole, A. P. Hedgeland, H. Jardine, W. Allison, J. Ellis, and G. Alexandrowicz, J. Phys.: Condens. Matter **24**, 104016 (2012).

[27] F. E. Tuddenham, H. Hedgeland, A. P. Jardine, B. A. J. Lechner, B. J. Hinch, and W. Allison, Surf. Sci. **604**, 1459 (2010).
[28] C. T. Chudley and R. J. Elliot, Proc. Phys. Soc. **77**, 353 (1960).
[29] H. Hedgeland, B. A. J. Lechner, F. E. Tuddenham, A. P. Jardine, W. Allison, J. Ellis, M. Sacchi, S. J. Jenkins, and B. J. Hinch, Phys. Rev. Lett. **106**, 186101 (2011).
[30] B. A. J. Lechner, A. S. de Wijn, H. Hedgeland, A. P. Jardine, B. J. Hinch, W. Allison, and J. Ellis, J. Chem. Phys. **138**, 194710 (2013).
[31] E. M. McIntosh, K. T. Wikfeldt, J. Ellis, A. Michaelides, and W. Allison, J. Phys. Chem. Lett. **4**, 1565 (2013).
[32] P. Fouquet, A. P. Jardine, S. Dworski, G. Alexandrowicz, W. Allison, and J. Ellis, Rev. Sci. Instrum. **76**, 53109 (2005).
[33] D. S. Sivia and J. Skilling, *Data Analysis: A Bayesian Tutorial* (Oxford University, New York, 2006).
[34] See Supplemental Material at http://link.aps.org/supplemental/10.1103/PhysRevB.89.121405 for a detailed description of the marginalized Bayesian method and its advantages.